Electronic Supplementary Information

Asymmetric Sandwich Structural Cellulose-based Film with Self-supported MXene and AgNW Layers for Flexible Electromagnetic Interference Shielding and Thermal Management

Bing Zhou,[a#] Qingtao Li,[a#] Penghui Xu,[a] Yuezhan Feng,[a*] Jianmin Ma,[b] Chuntai Liu,[a] Changyu Shen[a, c]

[a]*Key Laboratory of Materials Processing and Mold Ministry of Education, National Engineering Research Center for Advanced Polymer Processing Technology, Zhengzhou University, Zhengzhou, 450002, China.*

[b]*Key Laboratory for Micro-/Nano-Optoelectronic Devices, Ministry of Education, School of Physics and Electronics, Hunan University, Changsha 410022, China.*

[c]*State Key Laboratory of Structural Analysis for Industrial Equipment, Dalian University of Technology, Dalian, 116024, China.*

*Corresponding Author: E-mail: yzfeng@zzu.edu.cn (Y. Feng).

[#]B. Zhou and Q. Li contributed equally to this work (co-first authors).

Experimental Section

Preparation of CNF/MXene homogeneous films. Different amount of MXene nanosheets aqueous dispersion (2 mg/mL) was dropwise added to the CNF suspension (1 wt%) under continuous stirring. The mixture of CNF and MXene were continuously stirred for 12 h, and then filtered through vacuum-assisted filtration to obtain CNF/MXene composite film. The composite film was denoted CNF/MXene$_x$ where x stands for the weight ratio of MXene.

Fabrication CNF/MXene/AgNW homogeneous films. The as-prepared MXene dispersion and AgNW dispersion were added into CNF suspension under magnetic stirring for 12 h. The uniform suspension was filtered to form the CNF/MXene/AgNW composite film by the vacuum-assisted filtration. A series of CNF/MXene/AgNW film with a 50 wt % total filler content were prepared, to give different weight ratios of MXene/AgNW, 9:1, 7:3, 5:5, 3:7, and 1:9. The composite film was denoted CNF/MXene$_x$/AgNW$_y$ where x:y represent the MXene:AgNW mass ratio.

Fabrication CNF@MXene/AgNW sandwich films. First, a desired amount of CNF solution (25 mg solid content) was filtered to form the first layer. The mixture of AgNW and MXene with different weight ratios was stirred continuously for 12 h, and then filtered to obtain the inner mixing layer of MXene/AgNW. Finally, the CNF solution with equal amounts was added. After the water was filtered out, the filter cake with three layers was dried at room temperature for 48 h to a constant weight. The composite film was denoted CNF@MXene$_x$/AgNW$_y$ where x:y represent the MXene:AgNW mass ratio.

Characterizations. Morphology and microstructures were observed with a Zeiss MERLIN Compact field emission scanning electron microscope (FE-SEM, 10 kV), a Tecnai G2 F20 S-TWIN transmission electron microscopy (TEM, 200 kV), and a Bruker Dimension FastScan atom force microscopy (AFM, tapping mode). The electrical conductivity was measured by a four-probe resistivity meter (RTS-8, Guangzhou Four-Point Probe Technology Co., Ltd., China), and the corresponding conductivity was calculated using the equation[1] $\sigma = 1/(dR)$ (where d is the thickness of the film and R is the surface resistance). EMI shielding effectiveness (EMI SE) was measured with the vector network analyzer (Agilent Technologies N5244A, USA) within 8.2–12.4 GHz (X-band) and 18-26.5 GHz (K-band).

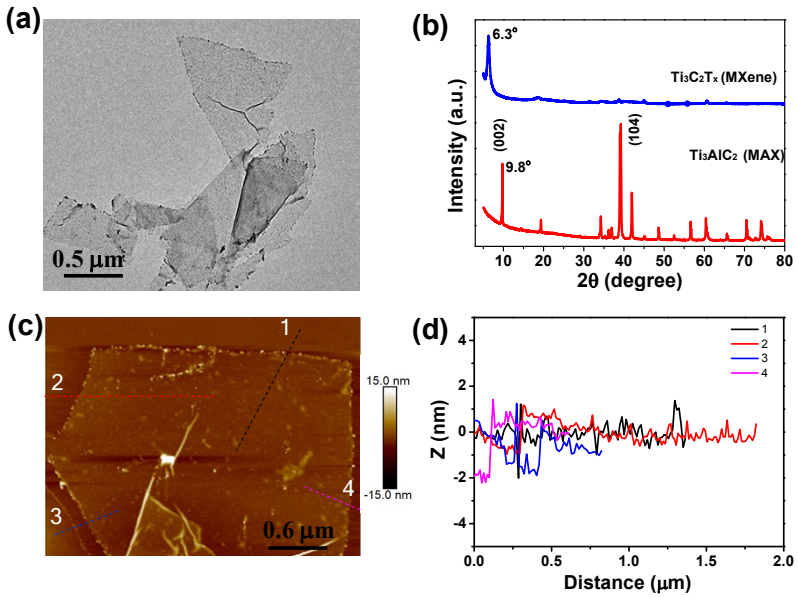

Fig. S1. (a) TEM image, (b) XRD spectrum, and (c) ANF image and (d) corresponding contour line of MXene.

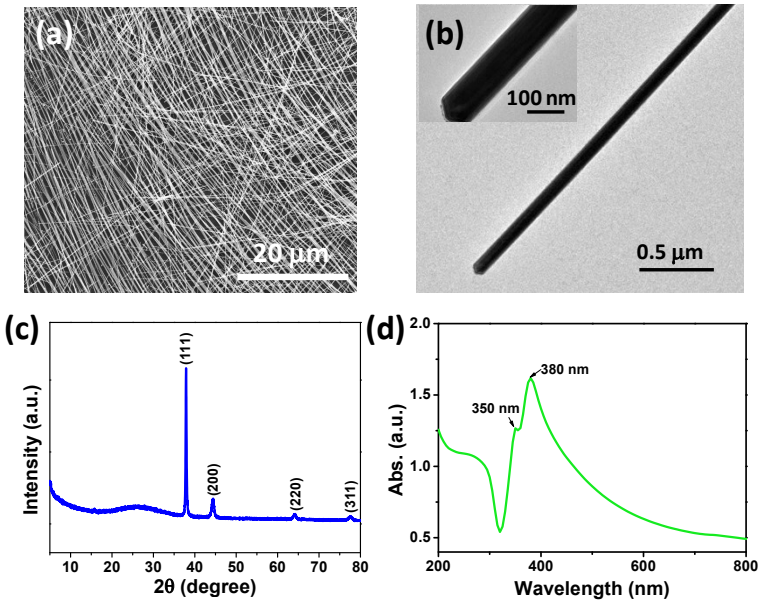

Fig. S2. (a) SEM image, (b) TEM image, (c) XRD spectrum, and (d) UV-vis spectrum of AgNW.

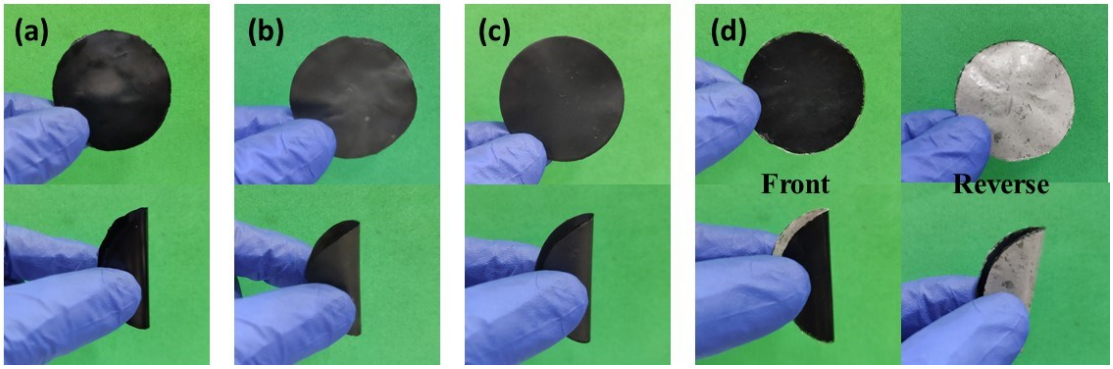

Fig. S3. Photographs of CNF/MXene, CNF/MXene/AgNW, CNF@MXene/AgNW and CNF@MXene@AgNW films.

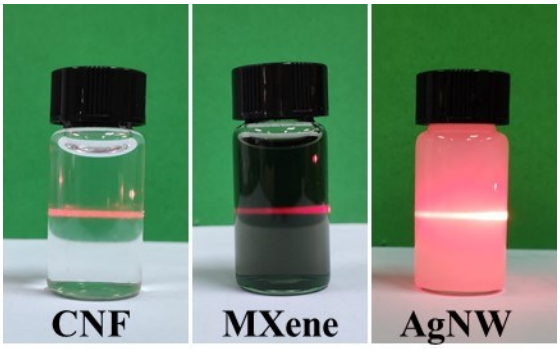

Fig. S4. Tyndall effect of CNF, MXene and AgNW aqueous solutions. Due to the abundant surficial groups (-OH, -O, -F), CNF and MXene reveal the outstanding dispersion in water. For AgNW, the residual PVP coating layer shown in Fig. S2b ensures the dispersion of AgNW in water.

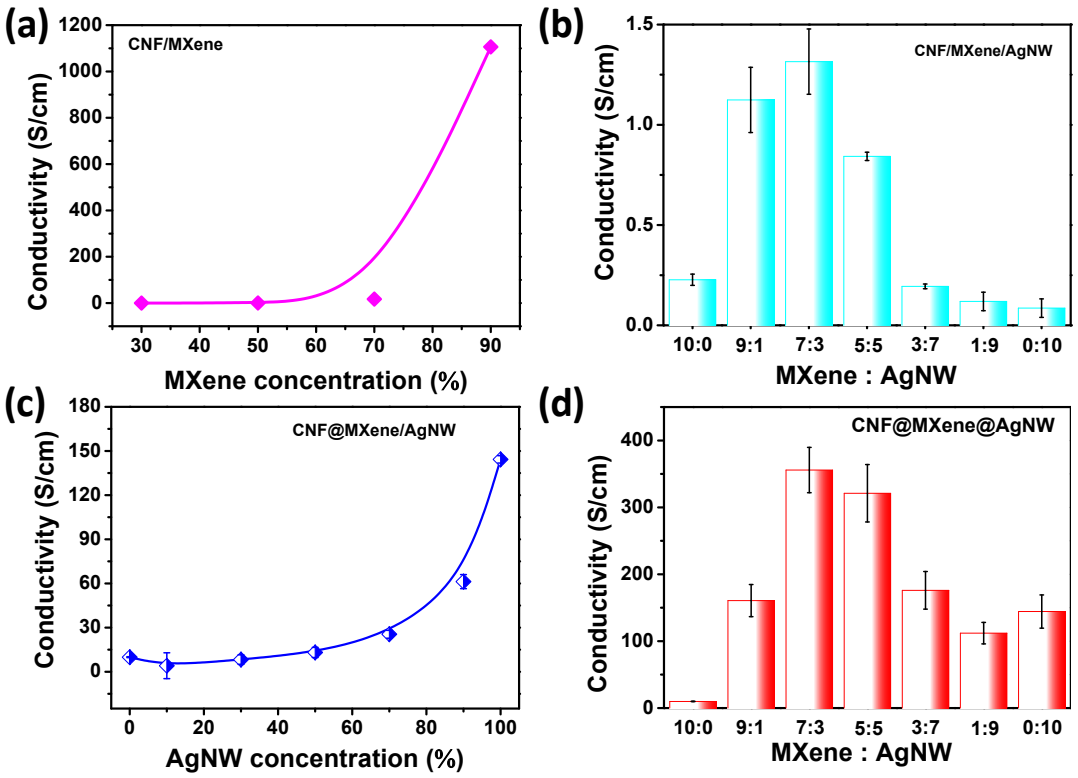

Fig. S5. Electrical conductivity of (a) CNF/MXene and (b) CNF/MXene/AgNW, (c) CNF@MXene/AgNW and (d) CNF@MXene@AgNW films.

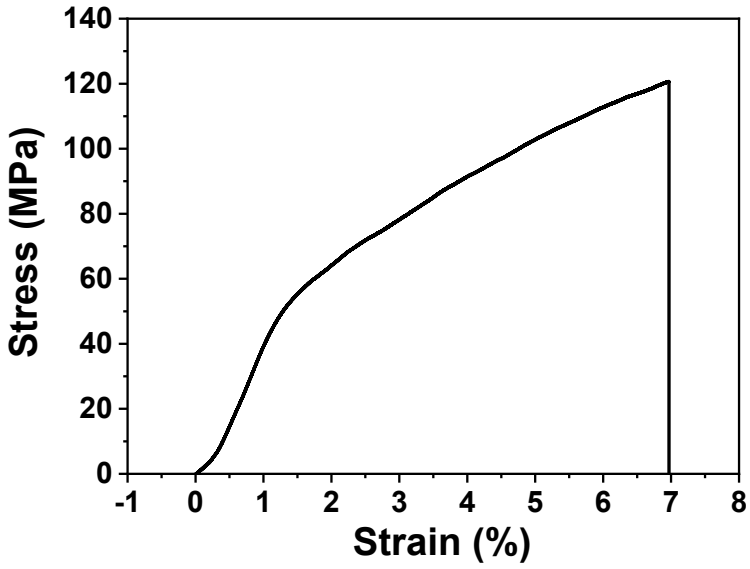

Fig. S6. Stress-strain curve of pure CNF film.

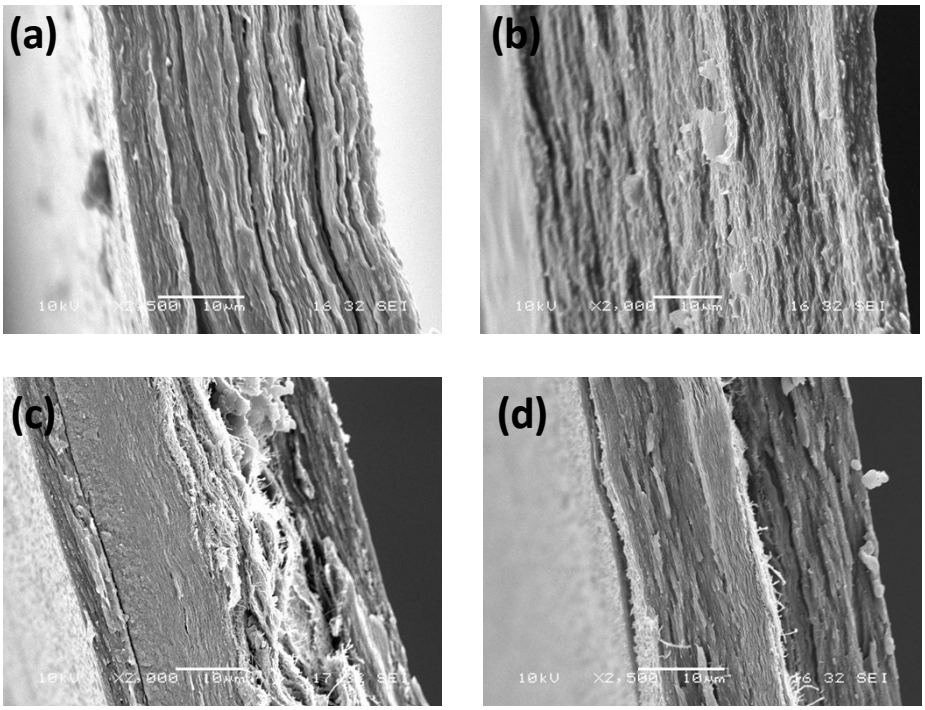

Fig. S7. SEM images of tensile fracture section for (a) CNF/MXene, (b) CNF/MXene/AgNW, (c) CNF@MXene/AgNW and (d) CNF@MXene@AgNW films

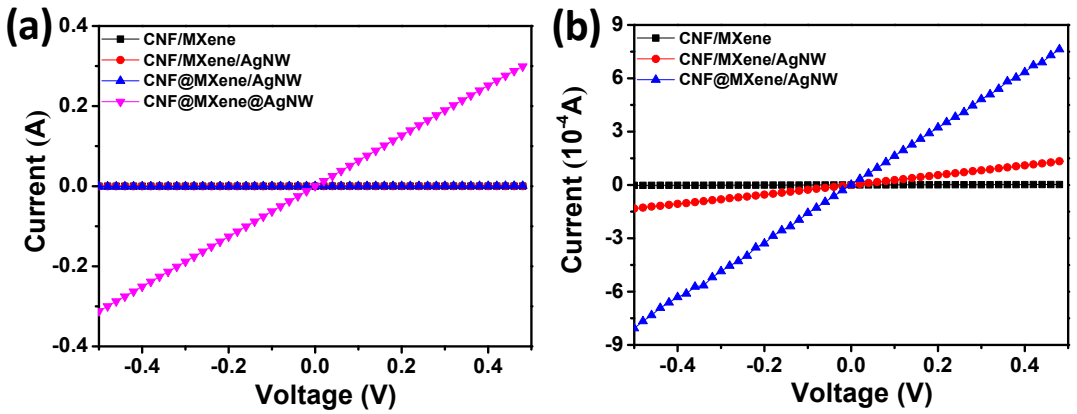

Fig. S8. I–V curves of CNF/MXene, CNF/MXene/AgNW, CNF@MXene/AgNW and CNF@MXene@AgNW films.

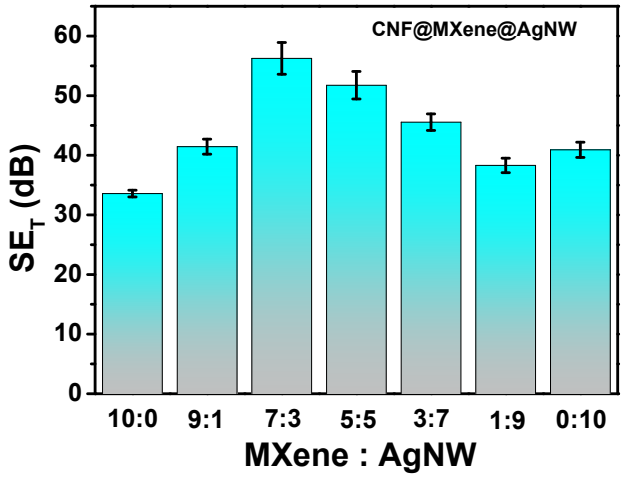

Fig. S9. Average SE_T values of CNF@MXene@AgNW film in X-band.

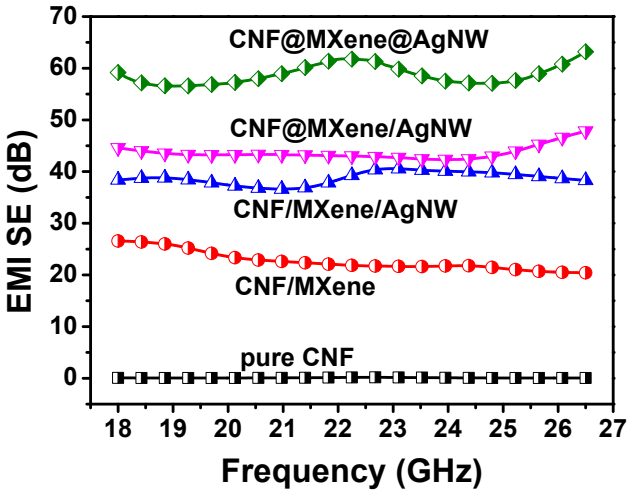

Fig. S10. EMI shielding performance of the samples in K-band.

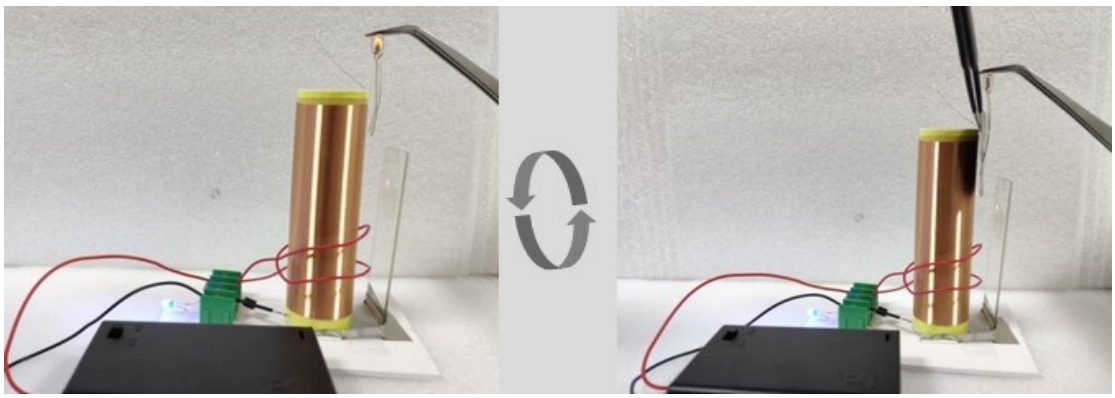

Fig. S11. A typical wireless power transmission system consisting of a DC power, transistors, transmitter coil, receiver coil, and light-emitting diode (LED) lights. When

the circuit is switched on, the direct current is converted to alternating current with the help of a transistor, creating an electromagnetic field. Subsequently, the LED is turned on due to the electromotive force generated in the receiver coil by the electromagnetic induction (left). When CNF@MXene@AgNW film is inserted between the two coils, the LED light is turned off, because the electromagnetic transmission is blocked (right and Movie S1). This simple experiment further proves that CNF@MXene@AgNW film has excellent EMI shielding performance.

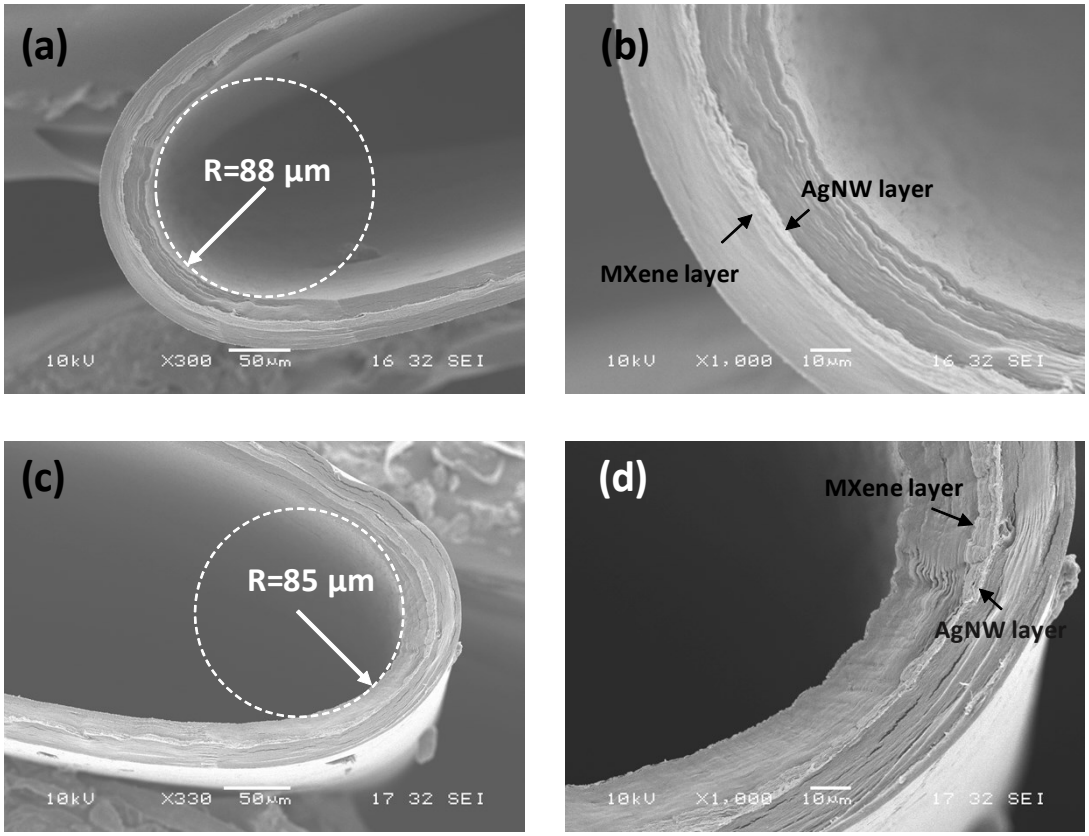

Fig. S12. SEM images of CNF@MXene@AgNW film in different bending directions.

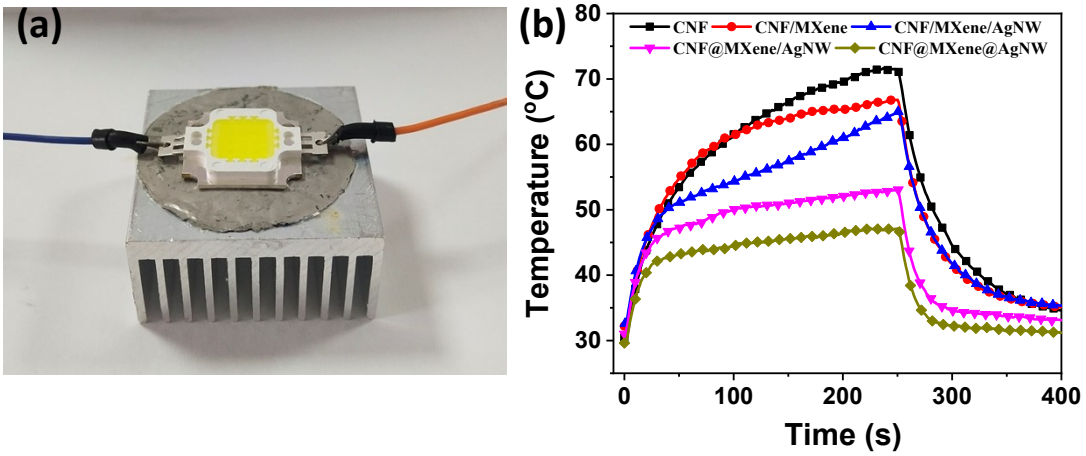

Fig. S13. (a) Photograph of LED light assembled on CNF@MXene@AgNW film and (b) temperature profiles of lighting LED with different films as TIMs.

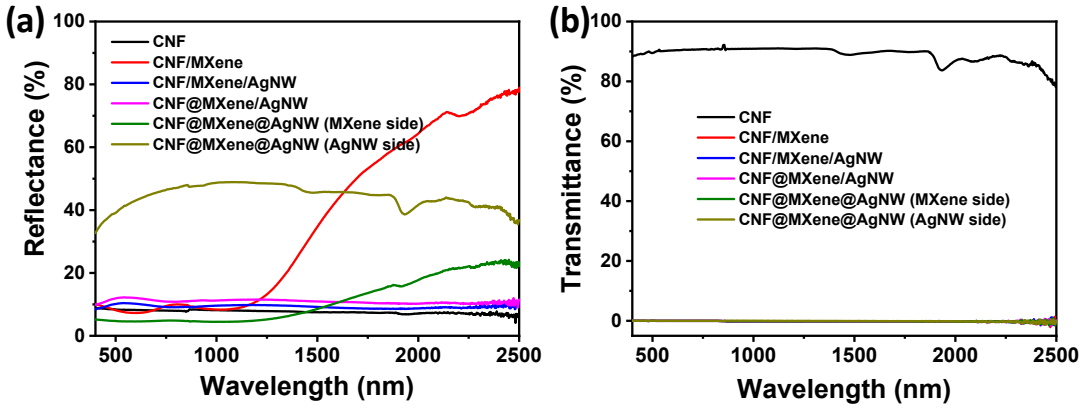

Fig. S14. UV-vis-NIR (a) reflection and (b) transmittance spectra of CNF, CNF/MXene, CNF/MXene/AgNW, CNF@MXene/AgNW and CNF@MXene@AgNW films.

Table S1. Comparison of EMI SSE/t versus thickness of CNF@MXene@AgNW film and other materials.

Sample	Materials	Thickness	Density	EMI	SSE/t	Ref.

		cm	g/cm^3	SE dB	(dB cm^2/g)	
CNT-based CPCs	MWNTs/WPU	0.23	0.07	35	2143	[1]
	MWNTs/PC	0.21	1.13	39	164	[2]
	MWNTs/ABS	0.11	1.14	40	318	[3]
	CNTs/CNF	0.015	1.70	35	1372	[4]
Graphene-based CPCs	rGO/PS	0.25	0.26	45.1	692	[5]
	rGO/PU	2	0.03	19.9	332	[6]
	rGO/PDMS	0.1	0.06	30	5000	[7]
	rGO/PMMA	0.024	0.76	19	1042	[8]
	rGO/PET	0.23	0.29	12.8	191	[9]
MXene-based CPCs	d-$Ti_3C_2T_x$/ANF	0.0017	1.26	28.54	13377	[10]
	$Ti_3C_2T_x$/TOCNF-50	0.0047	1.46	32.7	4761	[11]
	$Ti_3C_2T_x$/CNF	0.0047	1.93	24	2647	[12]
	$Ti_3C_2T_x$/PVA	0.5	0.01	28	5136	[13]
	CNT/MXene/CNF	0.0038	1.26	38.4	8020	[14]
	PVA/MXene	0.0027	1.74	44.4	9343	[15]
	CNF5@MXene4	0.0035	1.61	39.6	7029	[16]
	CNF@MXene@AgNW - 20%	0.0054	1.41	34.8	4570.5	**This work**
	CNF@MXene@AgNW - 50%	0.0035	1.5	55.9	10647.6	
	CNF@MXene@AgNW - 80%	0.0040	1.72	75.0	10901.6	

Table S2. Comparison of EMI SE and TC of CNF@MXene@AgNW film and previous literature.

Sample	Materials	Thickness mm	EMI SE dB	TC W/mK	Ref.
C	CNT/BN/rubber	1.4	32.52	0.25	[17]

NT-base	Fe_3O_4/CNT/ PVDF	1.1	33	0.62	[18]
	PVDF/CNT/Co-chain	0.3	35	1.39	[19]
	CNT/Ni/ PVDF	0.6	57	0.65	[20]
Graphene-based	GNPs/PS	3	33	4.72	[28]
	RGO/CNF	0.023	26.2	7.3	[20]
	M-rGO-WPU/cotton	1	48.1	2.13	[23]
	GNSs/CINAP/CE	2.7	55	4.13	[24]
	GNPs/rGO/epoxy	3	51	1.56	[25]
Metal-based	CuNWs-TAGA/epoxy	3	47	0.51	[26]
	GNS/Ni/PVDF	0.7	43.3	7.84	[27]
	Gn-SiCnw/PVDF	1.2	32.5	2.13	[28]
MXene-based	MXene/MMT	0.025	65	28.8	[29]
	MXene/cellulose	0.2	43	3.89	[30]
	MXene/PVA	0.027	44.4	4.57	[15]
	MXene-PVDF	2	48.75	0.767	[31]
	CNF@MXene@AgNW	0.035	55.9	15.53	**This work**

Supporting Movie 1. EMI shielding behavior of CNF@MXene@AgNW film, showing the film efficiently shields electromagnetic waves.

Reference

1. Z. Zeng, H. Jin, M. Chen, W. Li, L. Zhou and Z. Zhang, *Adv. Funct. Mater.*, 2016, **26**, 303-310.
2. S. Pande, A. Chaudhary, D. Patel, B. P. Singh and R. B. Mathur, *RSC Adv.*, 2014, **4**, 13839.
3. M. H. Al-Saleh, W. H. Saadeh and U. Sundararaj, *Carbon*, 2013, **60**, 146-156.

4. L. Zhang, B. Yang, J. Teng, J. Lei, D. Yan, G. Zhong and Z. Li, *J. Mater. Chem. C*, 2017, **5**, 3130-3138.

5. D.-X. Yan, H. Pang, B. Li, R. Vajtai, L. Xu, P.-G. Ren, J.-H. Wang and Z.-M. Li, *Adv. Funct. Mater.*, 2015, **25**, 559-566.

6. B. Shen, Y. Li, W. Zhai and W. Zheng, *ACS Appl. Mater. Interfaces*, 2016, **8**, 8050-8057.

7. Z. Chen, C. Xu, C. Ma, W. Ren and H. M. Cheng, *Adv. Mater.*, 2013, **25**, 1296-1300.

8. H. B. Zhang, Q. Yan, W. G. Zheng, Z. He and Z. Z. Yu, *ACS Appl. Mater. Interfaces*, 2011, **3**, 918-924.

9. J. Ling, W. Zhai, W. Feng, B. Shen, J. Zhang and W. Zheng, *ACS Appl. Mater. Interfaces*, 2013, **5**, 2677-2684.

10. F. Xie, F. Jia, L. Zhuo, Z. Lu, L. Si, J. Huang, M. Zhang and Q. Ma, *Nanoscale*, 2019, **11**, 23382-23391.

11. Z. Zhan, Q. Song, Z. Zhou and C. Lu, *J. Mater. Chem. C*, 2019, **7**, 9820-9829.

12. W. T. Cao, F. F. Chen, Y. J. Zhu, Y. G. Zhang, Y. Y. Jiang, M. G. Ma and F. Chen, *ACS Nano*, 2018, **12**, 4583-4593.

13. H. Xu, X. Yin, X. Li, M. Li, S. Liang, L. Zhang and L. Cheng, *ACS Appl. Mater. Interfaces*, 2019, **11**, 10198-10207.

14. W. Cao, C. Ma, S. Tan, M. Ma, P. Wan and F. Chen, *Nano-Micro Lett.*, 2019, **11**.

15. X. Jin, J. Wang, L. Dai, X. Liu, L. Li, Y. Yang, Y. Cao, W. Wang, H. Wu and S. Guo, *Chem. Eng. J.*, 2020, **380**, 122475.

16. B. Zhou, Z. Zhang, Y. Li, G. Han, Y. Feng, B. Wang, D. Zhang, J. Ma and C. Liu, *ACS Appl. Mater. Interfaces*, 2020, **12**, 4895-4905.

17. Y. Zhan, E. Lago, C. Santillo, A. E. Del Rio Castillo, S. Hao, G. G. Buonocore, Z. Chen, H. Xia, M. Lavorgna and F. Bonaccorso, *Nanoscale*, 2020, **12**, 7782-7791.

18. H. Cheng, S. Wei, Y. Ji, J. Zhai, X. Zhang, J. Chen and C. Shen, *Compos. A-Appl. S.*, 2019, **121**, 139-148.

19. X. Li, S. Zeng, S. E, L. Liang, Z. Bai, Y. Zhou, B. Zhao and R. Zhang, *ACS Appl. Mater. Interfaces*, 2018, **10**, 40789-40799.

20. B. Zhao, S. Wang, C. Zhao, R. Li, S. M. Hamidinejad, Y. Kazemi and C. B. Park, *Carbon*, 2018, **127**, 469-478.

21. Y. Guo, L. Pan, X. Yang, K. Ruan, Y. Han, J. Kong and J. Gu, *Compos. A-Appl. S.*, 2019, **124**, 105484.

22. W. Yang, Z. Zhao, K. Wu, R. Huang, T. Liu, H. Jiang, F. Chen and Q. Fu, *J. Mater. Chem. C*, 2017, **5**, 3748-3756.

23. Y. Wang, W. Wang, R. Xu, M. Zhu and D. Yu, *Chem. Eng. J.*, 2019, **360**, 817-828.

24. F. Ren, D. Song, Z. Li, L. Jia, Y. Zhao, D. Yan and P. Ren, *J. Mater. Chem. C*, 2018, **6**, 1476-1486.

25. C. Liang, H. Qiu, Y. Han, H. Gu, P. Song, L. Wang, J. Kong, D. Cao and J. Gu, *J. Mater. Chem. C*, 2019, **7**, 2725-2733.

26. X. Yang, S. Fan, Y. Li, Y. Guo, Y. Li, K. Ruan, S. Zhang, J. Zhang, J. Kong and

J. Gu, *Compos. A-Appl. S.*, 2020, **128**, 105670.

27. L. Liang, P. Xu, Y. Wang, Y. Shang, J. Ma, F. Su, Y. Feng, C. He, Y. Wang and C. Liu, *Chem. Eng. J.*, 2020, **395**, 125209.

28. C. Liang, M. Hamidinejad, L. Ma, Z. Wang and C. B. Park, *Carbon*, 2020, **156**, 58-66.

29. L. Li, Y. Cao, X. Liu, J. Wang, Y. Yang and W.Wang, *ACS Appl. Mater. Interfaces* 2020, **12**, 27350-27360.

30. D. Hu, X. Huang, S. Li and P. Jiang, *Compos. Sci. Technol.*, 2020, **188**, 107995.

31. K. Rajavel, S. Luo, Y. Wan, X. Yu, Y. Hu, P. Zhu, R. Sun and C. Wong, *Compos. A-Appl. S.*, 2020, **129**, 105693.